Utilizing Uncertainty of Time Series Prediction in Spectrum Sharing with Radar Systems

Su Pyae Sone* sone.supyae@oulu.fi
Janne Lehtomäki* janne.lehtomaki@oulu.fi
Zaheer Khan* zaheer.khan@oulu.fi
Kenta Umebayashi† ume_k@cc.tuat.ac.jp
Zunera Javed* zunera.javed@oulu.fi

†Department of Electrical and Electronic Engineering, Tokyo University of Agriculture and Technology (TUAT), Japan.
*Centre for Wireless Communications (CWC), University of Oulu, Finland.

2022 30th Telecommunications Forum (TELFOR) | 978-1-6654-7273-9/22/$31.00 ©2022 IEEE | DOI: 10.1109/TELFOR56187.2022.9983725

***Abstract*—Interference prediction with neural networks (NNs) can help in proactive resource management for spectrum sharing in 5.6 GHz radar bands. This can achieve high data rates for secondary users (SUs) of the shared spectrum and enhance the protection of the incumbent radar systems. The recently introduced efficient sharing and radar protection (ESRP) system with interference prediction used NN-based long short-term memory (LSTM) and Monte Carlo (MC) dropout to utilize the uncertainties in the interference from the access point (APs). Due to the random nature of radio propagation, the permissible probability of harmful interference at the radar (ε_p) for the ESRP system varies depending on the MC dropout and prediction intervals (PIs) which represents the amount of uncertainty captured in the system. In this work, we use a gated recurrent unit (GRU) which is simpler and faster than LSTM for interference prediction. We also investigate how the different MC dropout values can vary the parameter ε_p and improve the radar protection performance of the ESRP system. The results show that radar protection performance can increase by using GRU and the values of MC dropout play an important role in the ESRP system ensuring better radar protection with a small trade-off for throughput of the SUs which are the APs.**

***Keywords*—Dropout, Forecasting, GRU, LSTM, Neural Networks, Radars, Real Network Data, Time Series, WLAN.**

I. Introduction

Spectrum sharing between wireless communications and other wireless technologies is one solution to satisfy the demand for spectrum in both mobile cellular networks and enterprise wireless networks (WLANs). Among several spectrum sharing techniques, spectrum sharing in radar C-band, such as weather radars which can be found near urban areas, becomes popular for the enterprise WLAN networks operating in the 5.6 GHz band [1]. Although spectrum sharing with weather radar can benefit the communication of secondary enterprise WLAN users, protecting the incumbent radar system from any potential interference caused by the secondary users (SUs) is the priority for the spectrum sharing mechanism. Previously, the standardized dynamic frequency selection (DFS) and temporal DFS (DFS-T) are widely used for radar protection in the spectrum sharing with weather radar bands. The study [2] recommended using a cloud-assist Radio Environment Map (REM) repository radar protection system. Nevertheless, they all have the drawbacks of being inefficient due to their long spectrum sensing time [3], and delays in processing or reporting. Moreover, most of the weather radar rotations are quasi-periodic which are difficult to track in real-time [2] so that comprehensive radar protection is not guaranteed.

To address these limitations, the efficient sharing and radar protection (ESRP) system with aggregated interference prediction [4] is recently proposed. In the ESRP system, the NN-based LSTM prediction model is used to predict the degree of uncertainty in the aggregated interference at the radar caused by the SUs via the use of prediction intervals (PIs) generated with MC dropout. The predicted interference is compared with a tolerable threshold and the decision to remove certain SUs is executed in an advanced cloud-assist REM repository. The challenge of spectrum sharing with radar bands is that most radars, such as military radars and meteorological radars, have their critical functions and rules to follow. One main factor to consider for comprehensive primary radar protection is a parameter called the permissible probability of harmful interference at the radar (ε_p) which varies over a wide range depending on the application of a primary radar [5]. Our recent work [4] presented the relation between ε_p and the different percentages of PI set in the ESRP system with LSTM, and the minimum value of ε_p that can be used is 0.0006 with 99.9% PI. For some sensitive radars, the maximum allowable ε_p can be less than 0.0006 [5].

The spectrum sharing and radar protection mechanism for extremely sensitive radars in which the throughput of the SUs is better than the conventional protection system is required. One possible solution to improve the radar protection performance (reduce the ε_p value at which the ESRP system can be applied) is utilizing the uncertainty of the interference at the radar captured by the different MC dropout values of the NN-based training model in the ESRP system. Moreover, there is an abundance of literature using various NN-based interference predictions without considering the computational complexity of the models such as [6]. The previous work [7] stated that LSTM and GRU outperformed the other traditional recurrent NNs for sequence modeling, and GRU is similar to LSTM but with fewer operating gates. The computational complexity of the aggregated interference prediction in the ESRP system can also be reduced by using the GRU model. Therefore, the main contributions of this paper compared to our earlier work [4], include:

- We improve the radar protection performance of the ESRP system while the throughput of SUs is better than the conventional radar protection by using different MC dropout values.
- We use and evaluate the performances of the ESRP system with GRU and LSTM to show that GRU can

This work is supported by the Infotech Oulu, Academy of Finland 6Genesis Flagship, the European Commission in the framework of the H2020-EUJ-02-2018 project 5GEnhance, and by "Strategic Information and Communications R&D Promotion Programme (SCOPE)" of Ministry of Internal Affairs and Communications (MIC) of Japan.

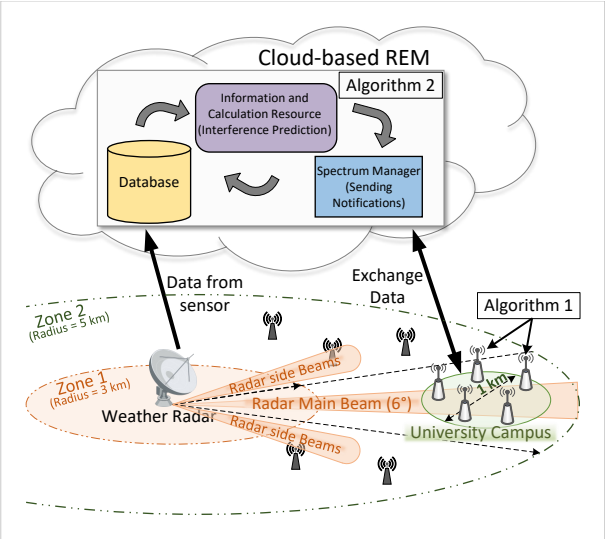

Fig. 1. Efficient sharing and radar protection (ESRP) system diagram

improve the radar protection performance for sensitive radars with less computational complexity.

II. The Models of Spectrum Sharing with a Weather Radar

A. Interference at the Radar

The collected real dataset, which comprises both network and physical layer data of APs deployed at the Linnanmaa campus of the University of Oulu, Finland, is used. As physical layer data, the total transmission power (TP) data of 7 APs each operating with a 5.6 GHz channel are collected. The TP data for all APs operating on 5.6 GHz are generated with the same multinomial model by using the number of connected users data explained in [4] and are used to calculate the aggregated interference at the radar. The aggregated interference at the radar caused by the secondary APs is modeled with the link budget calculation method. The simulation system is based on a ground-based meteorological radar operating at 5610 MHz and the Linnanmaa campus as shown in Fig 1. We consider downlink transmission of the APs with an additive white Gaussian noise (AWGN) channel and the other losses including building entry loss are considered in the link budget calculation. The ESRP system is mainly designed for the secondary APs to be able to share the radar channel even when the radar main beam is illustrated on them. Moreover, the interference at the radar is not only from the main lobe of radar but also from the side lobes.

The simulation model is designed by randomly generating the locations of K APs within the campus area since the exact locations of the APs do not significantly affect the aggregated interference on the radar. Moreover, the M active WLAN devices outside of the campus within zone 2 are modeled by using uniform distribution as in [3]. If the received and transmitted signal power from an i^{th} AP are defined as Pr_i and P_{ti}, the path loss between an i^{th} AP and the radar is $L_{PL,i} = \frac{P_{ti}}{Pr_i}$ and calculated as in [4]. We set the common building entry loss of an AP located in the campus as $L_{EL} = 11.5$ dB [8], the maximum radar gain as $G_{(max)} = 44$ dBi, the i^{th} AP gain as $G_{ti} = 6$ dBi, the bandwidths of radar channel and AP channel as $B_{radar} = 10$ MHz and $B_{AP} = 20$ MHz, respectively. Then, the interference power at the radar caused by the secondary APs under the radar main lobe at time t is [9]:

$$\Omega_{main} = \sum_{i=1}^{K} \frac{P_{ti} \cdot G_{ti} \cdot G_{radar(max)} \cdot B_{radar} \cdot \Phi_t}{B_{AP} \cdot L_{PL,i} \cdot L_{EL}}. \quad (1)$$

The TP of active WLAN devices outside of the campus at time t, $\Phi_{t(side)}$, is also generated uniformly with maximum power utilization of each device $k = 30\%$. Hence, the interference power at the radar caused by the side lobes is [3]:

$$\Omega_{side} = \sum_{j=1}^{M} \frac{P_{tj} \cdot G_{tj} \cdot G_{radar(min)} \cdot B_{radar} \cdot \Phi_{t(side)}}{B_j \cdot L_{PL,j} \cdot L_{EL}}, \quad (2)$$

where the minimum radar gain is defined as $G_{(max)} = 44$ dBi and the bandwidth of j^{th} active WLAN devices as $B_j = 20$ MHz. The aggregated interference from the main and the side lobes at the radar at time t is $\Omega_t = \Omega_{main} + \Omega_{side}$ which is used for prediction in the ESRP system. The maximum tolerable interference threshold of -104 dB is calculated as $Threshold = INR + N$, where, $N = -144(dBm) + 10\log_{10}(B_{radar})_{MHz} + \eta(dB)$, η = 10 dB is noise figure [9], and INR = -10 dB is interference to noise ratio [10].

B. Interference Forecasting Model

An LSTM network is used to predict the aggregated interference at the radar in our previous work [4] and a GRU network is used in this work for the benefit of faster prediction time. Both LSTM and GRU are the variance of recurrent NNs and are powerful tools for forecasting time series [7]. The closed-form expressions and algorithms for the LSTM and GRU layers can be found in [11]. If we denote all weights and bias (w, b) of the GRU layer as w_{GRU}, b_{GRU}, and the dense layer as w_{dense}, b_{dense}, the cost function of GRU (J_{GRU}) is the same as of LSTM (J_{LSTM}) described in [4] which is defined with mean absolute error (MAE) as

$$(\hat{w}_{GRU}, \hat{w}_{dense}, \hat{b}_{GRU}, \hat{b}_{dense}) = \arg\min_{w,b} \frac{1}{N} \sum_{t=1}^{N} |Y_t - \hat{Y}_t|, \quad (3)$$

where N is the number of samples in a predicted period and $\hat{w}_{GRU}, \hat{w}_{dense}, \hat{b}_{GRU}, \hat{b}_{dense}$ are the updated weights and bias of GRU and dense layers, respectively.

The generated data is for only weekdays between January 22 to February 22, 2020, with each data point at 10-minute intervals. The dataset is divided into 75% (15 days) training and 25% (5 days) testing datasets. The features-like grid training data structure is also used as in [4]. The optimized GRU model consists of 2 layers, each layer with 32 nodes. Each GRU layer is followed by the MC dropout layer with the probability ranging from [0.4 to 0.9] to prevent overfitting and to be able to compute the PIs of interference at the radar. Then, one dense layer is added as the output layer to directly output the predictions at the end. The Adam optimizer is also used in GRU training for its benefit of fast convergence compare to other optimizers [12]. In addition, the averaged accuracy values of 200 iterations are presented by considering the stochastic nature of the NNs.

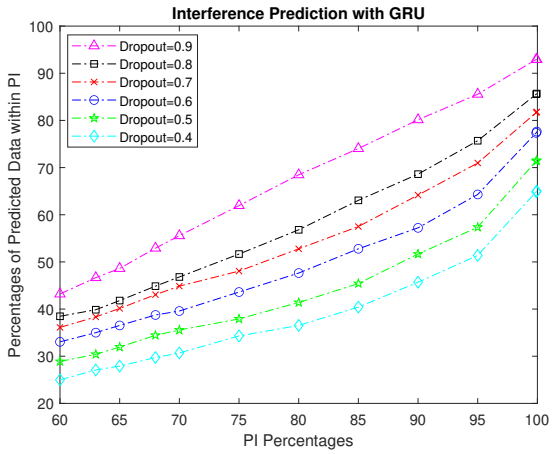

Fig. 2. True Data within forecasted prediction interval vs different dropout values of GRU for 1-hr FH

In the ESRP system, the computational time complexities (TCs) of LSTM and GRU can be compared in terms of theoretical big-O expressions and empirical measurements for a complete running time of a model [11]. For j^{th} layer, if we defined the number of input samples as N_{ij}, the number of hidden units as H_j, the number of output samples as N_{oj}, the number of time steps to train all training samples as T_{tr} and the number of layers as L, the theoretical TC expressions for training GRU and LSTM [11] are

$$\begin{aligned} GRU &: O((\sum_{j=1}^{L} 3N_{ij}H_j + 3H_j^2 + 2H_j + N_{oj}H_j)T_{tr}), \\ LSTM &: O((\sum_{j=1}^{L} 4N_{ij}H_j + 4H_j^2 + 3H_j + N_{oj}H_j)T_{tr}). \end{aligned} \tag{4}$$

Moreover, the empirical TC of the models are also estimated on the same hardware with the specifications: AMD Ryzen 7Pro 4750U CPU @1.7 GHz, 32 GHz RAM, x64 based processor in the same load condition. The statistical properties of the outputs, such as upper and lower limits of the predictions can be computed by using the MC dropout [13] as shown in Fig. 2. The range between actual upper and lower limits of the expected estimate with a probability with which the true value will be within that interval is called a prediction interval (PI).

III. Efficient Sharing and Radar Protection System

The efficient sharing and radar protection (ESRP) system is introduced in [4] to address the drawbacks of previous systems. The main goal of the ESRP system is to enable spectrum sharing with the radar channel regardless of the radar main beam's direction in zone 2 while ensuring comprehensive radar protection. The ESRP system maximizes $Throughput_j$, the averaged throughput of each connected user j at time t over total secondary APs and total periods, as well as minimizes P_{ot}, the aggregated interference points over the tolerable threshold of a radar, which are defined as follows:

$$Throughput_j = B_{AP} \cdot \log_2(1 + SINR) \cdot \phi_j, \tag{5}$$

where $SINR$ is the signal to interference and noise ratio at user j, and ϕ_j is the percentages of TP from the user j. Then, P_{ot} is denoted with the indicator function, $I_p(t)$, at time t as:

$$P_{ot} = \sum_{t=0}^{T} I_p(t) \quad where, I_p(t) = \begin{cases} 1, & \text{if } \Omega_t^R \geq Threshold, \\ 0, & \text{if } \Omega_t^R < Threshold, \end{cases} \tag{6}$$

which is limited by the permissible probability of harmful interference at the radar, $\varepsilon_p = \frac{P_{ot}}{T}$, as $Pr[\Omega_t^R \geq Threshold] \leq \varepsilon_p$ to consider the random nature of radio propagation [3]. The total number of time instances is denoted as T.

The ESRP system consists of two algorithms as shown in Fig 1. The simulation is done by assuming all connected APs are assigned to one main channel and a subordinate radar channel. Algorithm 1 at the APs' side is to stop the transmissions of the AP on the radar channel for the next period only when the notification from the REM is received. After the paused period, the APs can transmit on the radar channel again if no notification for the next period is received. The channel bonding method from [14] is used to bond the main and the radar channel for better throughput of the connected users of an AP. The cloud-based REM collects the information from the radar and the connected APs to predict the aggregated interference at the radar in the REM. Algorithm 2 at the cloud-based REM side calculates the amount of exceeded interference over the threshold as $R_I = I_{pre} - Threshold$, where I_{pre} is the predicted interference. If R_I is a non-zero positive value and the list of interference caused by each AP_i sorted in the descending order is defined as $[I_{\text{AP}_1}, I_{\text{AP}_2}, ..., I_{\text{AP}_K}]$, algorithm 2 finds the r number of APs such as $R_I \leq I_{\text{AP}_1} + I_{\text{AP}_2} + ... + I_{\text{AP}_r} < R_I + I_{\text{AP}_{r+1}}$. Then, the notifications are sent to r APs to stop sharing the radar channel. In this way, the radar channel is allocated efficiently between secondary APs not to exceed the tolerable threshold by utilizing the predicted interference. Previously, the different amounts of captured uncertainty are not considered in the interference perdition of the ESRP system. The main idea of this work is to utilize the highest prediction uncertainty (higher I_{pre} values) to ensure comprehensive radar protection by increasing R_I values.

IV. Performance Comparisons

The rotation time of the main beam of considered radar to illustrate on the same area is 60 seconds (rotating with 6° per sec). Hence, none of the APs located within zone 2 will be able to use the radar channel with the DFS system having the 60-sec channel availability check (CAC) period. In a real-time system, the measured interference at the radar at $t-1$ is fed back to cloud-based REM at every t. Hence, there are at least two time-step delays to stop the necessary APs from using the radar channel. Instead of waiting for the real-time feedback, we used time series of predicted interference at the radar in the ESRP system. The performances of different radar protection systems are compared based on two metrics: (a) $Throughout_j$, and (b) ε_p. The DFS system has the lowest averaged throughput per user and highest radar protection performance with $\varepsilon_p = 0$ since the secondary APs use only one main channel excluding the radar channel. The radar with ε_p less than 0.038 cannot use real-time radar protection due to its unavoidable delays in the system. The performances of the ESRP system with

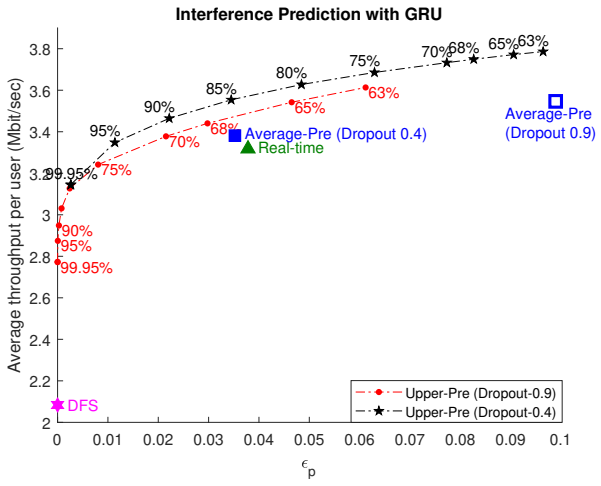

Fig. 3. Averaged throughput per user connected to each AP for different radar protection systems with GRU vs ϵ_p

LSTM and GRU are evaluated in two scenarios for different MC dropout values: 1) with various percentages of PI for upper limit prediction, and 2) with averaged prediction values in which the prediction uncertainty is not considered.

There is a trade-off between radar protection performance (ϵ_p) and the spectrum sharing performance ($Throughout_j$) in the ESRP system with an upper limit prediction. For both LSTM and GRU, the highest uncertainty captured in the upper limits of interference prediction (higher I_{pre} values) as in Fig. 2 makes sure to stop enough numbers of APs from sharing the radar channel resulting in higher R_I values not exceeding the interference threshold. The results showed that the ESRP system can also achieve $\epsilon_p = 0$ as in the DFS system but with higher averaged throughput per user if both LSTM and GRU use MC dropout 0.9 with 99.95% PI for aggregated interference prediction as shown in Fig. 3. Hence, the simple method, adjusting MC dropout values and percentages of PI for the upper limit prediction to capture the highest uncertainty, is proposed in this work to improve the radar protection performance regardless of whether LSTM or GRU is used while the averaged throughput per user is better than the conventional radar protection system. Moreover, the recorded empirical TC of 1-hr FH for GRU is 1063.28 seconds while TC for LSTM is 1232.86 seconds. Therefore, using the GRU with MC dropout 0.9 for upper limit prediction of 99.95% PI in the ESRP system is the optimal setting for the sensitive radars in terms of computational TC, radar protection, and spectrum sharing performances. However, the random nature of radio propagation and sudden changes in the transmission traffic of the SUs become the main challenges to maintaining constant radar protection performance while sharing the radar channel spectrum.

V. Conclusion

Spectrum sharing between radars in the 5.6 GHz band and wireless enterprise networks can help in providing higher capacity. A machine learning-driven technique, the efficient sharing and radar protection (ESRP) system, has been introduced recently. One main challenge of sharing a spectrum with radar is that most of the radar systems have a different permissible probability of harmful interference at the radar (ϵ_p) values to follow. We have proposed the simple method, adjusting the MC dropout value in the LSTM and GRU models to consider the highest prediction uncertainty, to improve the radar protection performance of the ESRP system for sensitive radars. The performances of different radar protection systems such as DFS, real-time, ESRP with averaged prediction, and ESRP with upper limit prediction systems are also compared in both spectrum sharing and radar protection aspects. We also showed that the ESRP system with the upper limit prediction of GRU is optimal for sensitive radars which have a very small allowable ϵ_p value in terms of computational TC, radar protection, and spectrum sharing performances.

References

[1] F. Paisana, N. Marchetti, and L. A. DaSilva, "Radar, TV and cellular bands: Which spectrum access techniques for which bands?," *IEEE Communications Surveys & Tutorials*, vol. 16, no. 3, pp. 1193–1220, 2014.

[2] Z. Khan, J. J. Lehtomäki, R. Vuohtoniemi, E. Hossain, and L. A. DaSilva, "On opportunistic spectrum access in radar bands: Lessons learned from measurement of weather radar signals," *IEEE Wireless Communications*, vol. 23, no. 3, pp. 40–48, 2016.

[3] M. Tercero, K. W. Sung, and J. Zander, "Impact of aggregate interference on meteorological radar from secondary users," in *Proceedings of IEEE Wireless Communications and Networking Conference*, pp. 2167–2172, IEEE, 2011.

[4] S. P. Sone, J. Lehtomäki, Z. Khan, K. Umebayashi, and Z. Javed, "Proactive radar protection system in shared spectrum via forecasting secondary user power levels," *IEEE Access*, pp. 1–1, 2022.

[5] E. Obregon, K. W. Sung, and J. Zander, "Is spectrum sharing in the radar bands commercially attractive? - a regulatory and business overview," *Transactions on Emerging Telecommunications Technologies*, vol. 27, no. 3, pp. 428–438, 2016.

[6] Y. Zhao, L. Shi, X. Guo, and C. Sun, "Aggregate interference prediction based on back-propagation neural network," in *Proceedings of IEEE International Symposium on Dynamic Spectrum Access Networks (DySPAN)*, pp. 1–5, IEEE, 2018.

[7] J. Chung, C. Gulcehre, K. Cho, and Y. Bengio, "Empirical evaluation of gated recurrent neural networks on sequence modeling," in *Proceedings of NIPS Workshop on Deep Learning*, NeurIPS, December 2014.

[8] Report, "Compilation of measurement data relating to building entry loss," *ITU-R 2346-2, Geneva*, 2017.

[9] Recommendation, "Procedures for determining the potential for interference between radars operating in the radiodetermination service and systems in other services," *ITU-R M.1461-2, Geneva*, 2018.

[10] J. M. Peha, "Cellular systems and rotating radar using the same spectrum," in *Proceedings of International Symposium on Advance Radio Technologies (ISART)*, NTIA, July 2011.

[11] S. P. Sone, J. J. Lehtomäki, and Z. Khan, "Wireless traffic usage forecasting using real enterprise network data: Analysis and methods," *IEEE Open Journal of the Communications Society*, vol. 1, pp. 777–797, 2020.

[12] C. Zhang and P. Patras, "Long-term mobile traffic forecasting using deep spatio-temporal neural networks," in *Proceedings of 18th ACM International Symposium on Mobile Ad Hoc Networking and Computing (ISMNC)*, pp. 231–240, ACM, June 2018.

[13] Y. Gal and Z. Ghahramani, "Dropout as a bayesian approximation: Representing model uncertainty in deep learning," in *Proceedings of International Conference on Machine Learning (ICML)*, pp. 1050–1059, Machine Learning Research, 2016.

[14] Z. Khan, J. Lehtomäki, S. Scott, Z. Han, M. Krunz, and A. Marshall, "Distributed and coordinated spectrum access methods for heterogeneous channel bonding," *IEEE Transactions on Cognitive Communications and Networking*, vol. 3, no. 3, pp. 267–281, 2017.